

The impact of secular resonances on habitable zones in circumstellar planetary systems of known binary stars

Ákos Bazsó

Institute for Astrophysics, University of Vienna
Türkenschanzstraße 17, A-1180 Vienna, Austria

bazso@astro.univie.ac.at

Elke Pilat-Lohinger

Institute for Astrophysics, University of Vienna
Türkenschanzstraße 17, A-1180 Vienna, Austria

elke.pilat-lohinger.univie.ac.at

Siegfried Eggl

IMCCE, Observatoire de Paris
77 Avenue Denfert-Rochereau, F-75014 Paris, France

Barbara Funk

Institute for Astrophysics, University of Vienna
Türkenschanzstraße 17, A-1180 Vienna, Austria

and

David Bancelin

Institute for Astrophysics, University of Vienna
Türkenschanzstraße 17, A-1180 Vienna, Austria

Received _____; accepted _____

ABSTRACT

We present a survey on binary star systems with stellar separations less than 100 astronomical units. For a selection of 11 binaries with a detected (giant) planet in circumstellar motion we determine the conditions that would allow additional planets to be present inside or nearby the habitable zone (HZ) of the host star. First we calculate the three-body HZ for these systems, in order to investigate the dynamics of bodies in those regions. After adding the giant planet's influence the final HZ is considerably modified in particular by mean motion and secular resonances. We apply a semi-analytical method to determine the locations of linear secular resonances, which is based on finding the apsidal precession frequencies of the massive bodies. For very close-in giant planets we also take the general relativistic precession of the pericenter into account. Our results demonstrate that there is a qualitative difference in the dynamics whether the giant planet is located exterior or interior to the HZ. An exterior giant planet is more likely to cause a secular resonance than an interior planet. Exterior planets play an important role for the HZ by enforcing highly eccentric orbits on potentially habitable planets. For interior planets generally we do not find a secular resonance in the Newtonian framework, but the general relativistic precession introduces another source for a secular resonance. In 7 out of 11 systems secular resonances play a role. We compare our semi-analytical method to various purely analytical models, and show that it is more accurate in determining the location of secular resonances.

Subject headings: binaries: general — celestial mechanics — habitable zone — secular resonance — stars: individual (...)

1. INTRODUCTION

Extrasolar planets (exoplanets) orbiting other stars exist in a large variety of different configurations. Some exoplanets orbit their host star with periods of only a few days, e.g. the Hot Jupiters (see Beaugé & Nesvorný 2012; Naoz et al. 2012). Other exoplanets were observed on wide orbits at large distances from their host star, e.g. HR 8799 (Marois et al. 2008); however, their formation mechanism is still poorly understood (Dodson-Robinson et al. 2009; Vorobyov 2013). An important point is that exoplanets are not exclusive companions to single stars, but also binary and multiple stars can host planetary objects (Campbell et al. 1988; Zucker et al. 2002). Although exoplanets in binary and multiple star systems have been found, it is not clear whether or not these environments are more hostile for the presence of planets than single stars (Boss 2006; Bromley & Kenyon 2015; Jang-Condell 2015). For instance, Armstrong et al. (2014) derived from the *Kepler* data an occurrence rate of coplanar circumbinary planets that is similar to the rate for single stars.

Binary and multiple star systems are frequent in the solar neighbourhood, observational surveys (Duquennoy & Mayor 1991; Raghavan et al. 2010; Tokovinin 2014) derived a fraction of up to 45 %. Naturally, not all of those systems are hosting planets, but recent estimates on the multiplicity of exoplanet host stars (Raghavan et al. 2006, 2010; Mugrauer & Neuhäuser 2009; Roell et al. 2012) yield the percentage of double stars to be 10–15 %, while multiple systems make up for about 2 %.

Known exoplanets in binary star systems can be divided into three classes of motion from a dynamical point-of-view, of which S-type (Rabl & Dvorak 1988) and P-type (Dvorak et al. 1989) are the most important cases. S-type planets are circumstellar planets; they orbit one component of the binary star system, just as a planet would orbit a single star. P-type planets are circumbinary planets that orbit both stars in some distance.

Rabl & Dvorak (1988) established an empirical formula for the size of the region where stable circumstellar planetary motion in an eccentric binary system (with equal masses) can occur. Holman & Wiegert (1999) extended this analysis by including a variable mass ratio of the binary in the S- and P-type cases. Pilat-Lohinger & Dvorak (2002) investigated the influence of a non-zero initial eccentricity on the orbital stability of an S-type planet in binary star systems. They applied the Fast Lyapunov Indicator (FLI, see Froeschlé et al. 1997), a method to detect chaos in some region of the phase space, to determine the boundary of the stable region. More recently, Jaime et al. (2014) formulated radiative and dynamical constraints on circumstellar and circumbinary HZs. They determined regions of stable and non-intersecting planetary orbits in eccentric binary star systems by searching for invariant loops, which result in exact stability criteria since they are backed by integrals of motion.

Although the orbital stability of exoplanets is an intriguing topic in itself, here we are more interested in exoplanets inside or close to the habitable zone (HZ) in binary star systems. Orbital stability is not the only prerequisite for long-term habitability. Substantial changes in insolation that are due to variations in planetary orbits have to be taken into account as well. Therefore, we need to consider the effect of both mean-motion resonances (MMR, involving orbital frequencies) and secular resonances (SR, related to apsidal frequencies) (see Murray & Dermott 1999; Beaugé et al. 2012) on the terrestrial planet’s orbit. Here, we focus on secular resonances, since secular resonances can strongly modify the planet’s eccentricity which can have a dramatic influence on a planet’s habitability.

In this work we investigate binary star systems with a known giant planet in order to determine how a hypothetical (terrestrial) planet in the HZ would react to secular perturbations from the giant planet and the companion star. The next section 2 presents the binary star systems selected for our investigation, and explains how we determined

the habitable zones for those systems. In section 3 we give a short summary of the semi-analytical method introduced by Pilat-Lohinger et al. (2016) (hereafter referred to as EPL16) that allows to calculate accurately the location of SR in binary star systems. We present the results of the survey in section 4, where we also describe two systems in more detail. Finally, we discuss the semi-analytical method and compare its performance relative to some purely analytical models in section 5.

2. THE INVESTIGATED SYSTEMS

As of January 2016 76 binary star systems with 109 planets had been discovered, as well as 19 multiple star systems with 24 planets. Out of this 76 binary systems 59 are of S-type and 17 of P-type.

2.1. Selection of Systems

For this survey we have selected binary star systems with (projected) separations $a_B \leq 100$ AU; these binary stars have typical orbital periods of less than 1000 years (for stellar mass objects). At this separation the secondary star will influence planet formation by truncating the protoplanetary disc of the primary star (Kley & Nelson 2010; Jang-Condell 2015). In addition, the secular dynamics of any successfully formed planets in the system will strongly depend on the separation between the two stars (Quintana et al. 2007; Pilat-Lohinger et al. 2016). Given the above constraints on stellar separation, 15 S-type candidates remained in our sample. This list includes α Centauri, a close binary with a distant third stellar companion. We discarded the Kepler-296 system from the list, because it is a compact multiplanetary system with 5 planets within 0.27 AU of the host star (Rowe et al. 2014; Barclay et al. 2015). The OGLE-2008-BLG-092L (Poleski et al. 2014)

and OGLE-2013-BLG-0341L (Gould et al. 2014) systems were rejected due to insufficient data regarding the orbits of the companion star and the planet. We also note that in the Kepler-420 (KOI-1257) system the giant planet and secondary star have such high eccentricities (Santerne et al. 2014) that the dynamically stable zone around the host star is necessarily devoid of additional planets.

In the end, 11 systems remained to be investigated. Table 1 provides an overview of their properties, the basic parameters such as stellar masses and the planet’s minimum mass ($M_P = m \sin i$), as well as the semi-major axes and eccentricities for the binary and the planet. This table—in connection with Figure 1—summarises the main physical and dynamical aspects of the systems of interest.

It becomes evident from Table 1 that—except for α Cen Bb—all planets have rather high (minimum) masses of the order of 1 Jupiter mass. As a consequence these planets could efficiently perturb additional (hypothetical) Earth-mass planets in the systems.

In eight of the eleven systems the stars have very different masses with mass ratios $\mu < 0.4$ ($\mu = M_B/(M_A + M_B)$), only for α Cen the stars have almost equal masses with a mass ratio of $\mu = 0.54$. In most of the cases the secondary star is an M-dwarf, notable exceptions are again α Cen with a G2V companion (Endl et al. 2015), Kepler-420 with a K6V companion (Santerne et al. 2014), and Gliese 86 for which the secondary is a white dwarf (Fuhrmann et al. 2014). Also note that HD 177830 is the only system with two planets, in all other cases only a single planet has been discovered so far.

Figure 1 presents a schematic overview of the binary star systems. The disk sizes for the primary (host) and secondary star indicate their masses (cf. Table 1), the box in the top left corner displays four typical cases for M-, K-, G-, and F-type stars. A large dashed horizontal bar extending from the left marks the host star’s dynamical stability zone, beyond which it can no longer host S-type planets (Holman & Wiegert 1999; Pilat-Lohinger & Dvorak

Table 1: List of binary star systems ordered by decreasing stellar separation a_B .

System	Masses			Semi-major axes		Eccentricities		Reference
	M_A (M_\odot)	M_B (M_\odot)	M_P (M_J)	a_B (AU)	a_P (AU)	e_B	e_P	
94 Cet Ab	1.34	0.90	1.68	100	1.42	0.26	0.3	(1)
HD 177830 Ab	1.47	0.23	1.49	97	1.22	0.20 ^a	0.001	(2)
HD 177830 Ac	0.15	...	0.51	...	0.349	(2)
GJ 3021 Ab	0.90	0.13	3.37	68	0.49	0.20 ^a	0.51	(3)
τ Boo Ab	1.30	0.40	4.13	45	0.05	0.20 ^a	0.02	(4)
HD 126614 Ab	1.15	0.32	0.38	36.2	2.35	0.50 ^b	0.41	(5)
α Cen Bb	1.11	0.93	0.004	23.4	0.04	0.52	0.0	(6)
HD 41004 Ab	0.70	0.40	2.54	23	1.64	0.20 ^a	0.2	(7)
HD 196885 Ab	1.33	0.45	2.98	21	2.60	0.42	0.48	(8)
γ Cep Ab	1.40	0.41	1.85	20.2	2.05	0.41	0.05	(9)
Gliese 86 Ab	0.83	0.49	4.01	19	0.11	0.40	0.05	(10)
Kepler-420 Ab	0.99	0.70	1.45	5.3	0.38	0.31	0.772	(11)

Note. — The planet hosting star is indicated by the capital letter A or B . Stellar masses are in units of solar masses (M_\odot), while planet masses are given in Jupiter masses (M_J). The semi-major axes are given in astronomical units (AU).

^aassumed eccentricity

^bupper limit for stable planetary motion

References. — (1) Roell et al. (2012), (2) Meschiari et al. (2011), (3) Chauvin et al. (2007), (4) Roberts et al. (2011), (5) Howard et al. (2010), (6) Dumusque et al. (2012); Endl et al. (2015), (7) Zucker et al. (2004); Funk et al. (2015), (8) Chauvin et al. (2011), (9) Endl et al. (2011), (10) Fuhrmann et al. (2014), (11) Santerne et al. (2014).

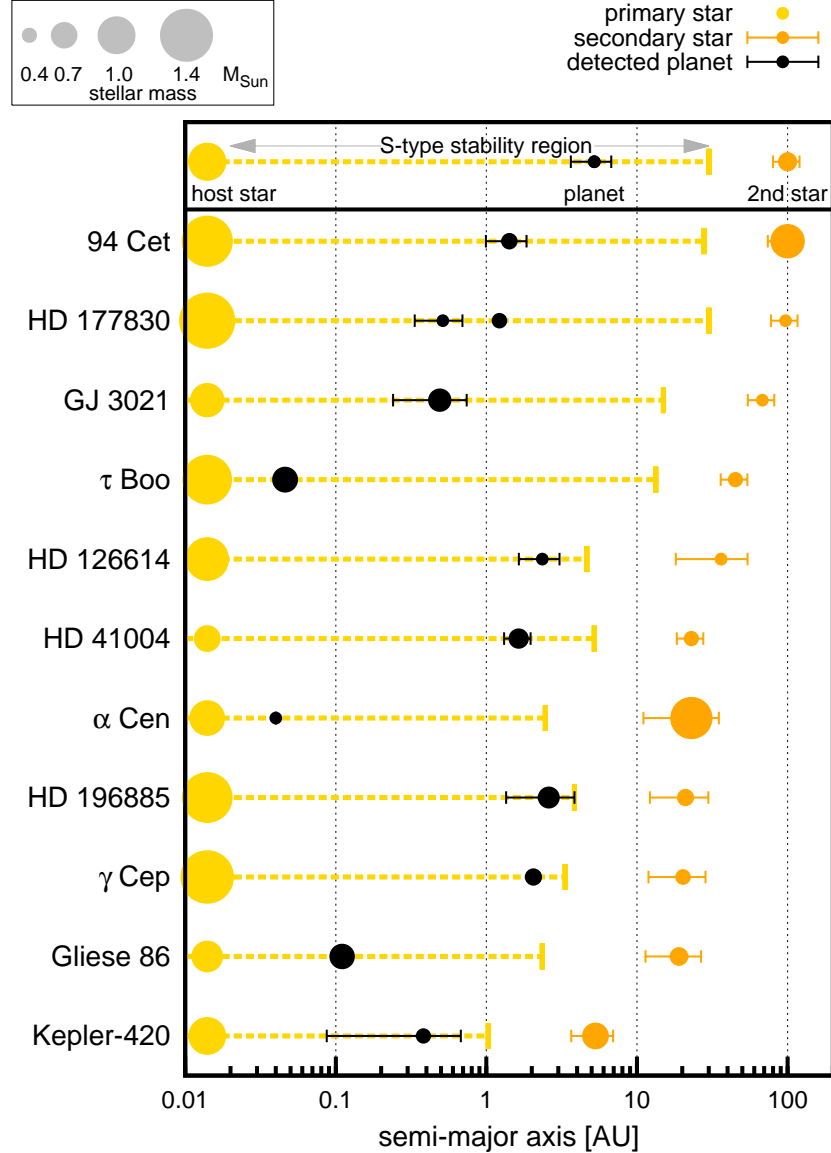


Fig. 1.— Schematic overview of the binary star systems. The size of the disk for the primary and secondary star indicates their masses according to the scale in the top left corner; the planet disk is not to scale. Continuous horizontal error bars show the minimum and maximum distances of the respective objects, which are related to the eccentricity. The large dashed bar marks the region for stable S-type motion about the host star in the respective system.

2002). As opposed to this, the secondary star might harbour S-type planets in a subregion outside this zone. We indicate the eccentricities of the secondary star and the planet with horizontal error bars having the colour of the respective object.

2.2. Habitable Zone

The classical habitable zone was defined for a single Earth-like planet on a circular orbit around a single star (Kasting et al. 1993; Kopparapu et al. 2013). Various attempts have been made to extend the concept of the HZ to binary stars, among others by Eggl et al. (2012); Kaltenegger & Haghjipour (2013); Cuntz (2014); Jaime et al. (2014). The major point is to take into account the insolation onto the planet from both stars as a function of their luminosity, orbital parameters, as well as the changes in the planet’s orbit.

Following Eggl et al. (2012) we can distinguish three different types of HZs for S-type planets, based on the maximum and minimum habitable insolation limits S_{in} and S_{out} :

PHZ permanent HZ (or classical HZ), where the planet is always within a prescribed annulus defined by the insolation limits for the binary star system: $S_{\text{in}} \geq S \geq S_{\text{out}}$.

EHZ extended HZ, where the planet is almost always within the limits, i.e. more specifically the inequality $S_{\text{in}} - \sigma \geq \langle S \rangle \geq S_{\text{out}} + \sigma$ holds for the time-averaged effective insolation $\langle S \rangle$ from both stars, where σ^2 is its variance.

AHZ average HZ, where the planet is on average within the limits: $S_{\text{in}} \geq \langle S \rangle \geq S_{\text{out}}$.

The classical conditions for habitability lead to the most conservative value, the PHZ. Here, the temporal variations in the planet’s orbit and the corresponding changes in insolation are tracked and evaluated rigorously in order to never exceed habitable limits. For the AHZ the constraints are more relaxed, and the planet can spend a considerable fraction of its

orbital period outside the classical HZ. Alternative methods for calculating the habitable zones in binary star systems, that neglect planetary orbit variations, were proposed by Kaltenegger & Haghjhipour (2013) and Cuntz (2014), which would yield slightly different results.

Table 2 summarises the extent of the various types of HZ. For each type we indicate the inner and outer border (in AU), calculated for a three-body HZ (two stars and a test planet), which neglects the influence of the giant planet. Taking into account the giant planet would lead to a truncation of the HZ in some cases (see Figure 2). Besides the HZ, the table also indicates the border of the stability region for S-type motion. We have determined the boundary for regular S-type motion around the host star for each individual system by using the Fast Lyapunov Indicator (FLI) as presented in Pilat-Lohinger & Dvorak (2002). The last column shows the location of the linear secular resonance with the detected planet (see section 4); the missing entries for 4 systems mean that there is no such resonance (at least not in the region of interest).

In Figure 2, we plot the three-body HZ as hatched boxes, whereas the effective four-body HZ are coloured in blue. Including the giant planet’s influence leads to a truncation of the HZ in some cases due to stability issues. Additionally, mean-motion resonances with the giant planet also occur at various locations inside the HZ, which we do not show in the figure. For the systems γ Cep and Kepler-420 the HZ lies outside the stable region, this is indicated by a dashed red border around the HZ. The black dots show the location of the detected planets, where the horizontal error bars (extending from periastron to apoastron) visualise the planet’s eccentricity. Finally, a cross symbol marks the location of the linear secular resonance. For HD 177830 the two planets cause a secular resonance at least at two locations, these are marked in Figure 2 and given in Table 2. In the two cases where the secular resonance lies inside the HZ (HD 177830 and α Cen) its influence is

Table 2: Extension of the three-body habitable zone (inner and outer borders), outer limit of the stability region, and location of the secular resonance in the binary star systems.

System	AHZ		EHZ		PHZ		Stability limit	Resonance location
	inner	outer	inner	outer	inner	outer		
94 Cet	1.84	3.11	1.85	3.08	1.86	3.05	27.90	...
HD 177830	2.34	4.30	2.35	4.25	2.37	4.21	30.02	2.11, 3.77
GJ 3021	0.81	1.40	0.81	1.39	0.81	1.39	14.96	...
τ Boo	1.67	2.84	1.68	2.80	1.70	2.75	13.30	0.45
HD 126614	1.09	1.90	1.12	1.82	1.15	1.75	4.63	0.91
α Cen	0.72	1.26	0.74	1.21	0.76	1.16	2.45	1.16
HD 41004	0.79	1.40	0.81	1.35	0.83	1.30	5.20	0.37
HD 196885	2.06	3.53	2.17	3.23	2.36	2.97	3.84	1.11
γ Cep	4.17	5.70	4.36	5.70	4.79	5.70	3.33	0.78
Gliese 86	0.63	1.10	0.63	1.10	0.63	1.10	2.34	...
Kepler-420	0.95	1.67	0.98	1.52	0.99	1.33	1.02	...

Note. — All numbers in this table are in astronomical units (AU).

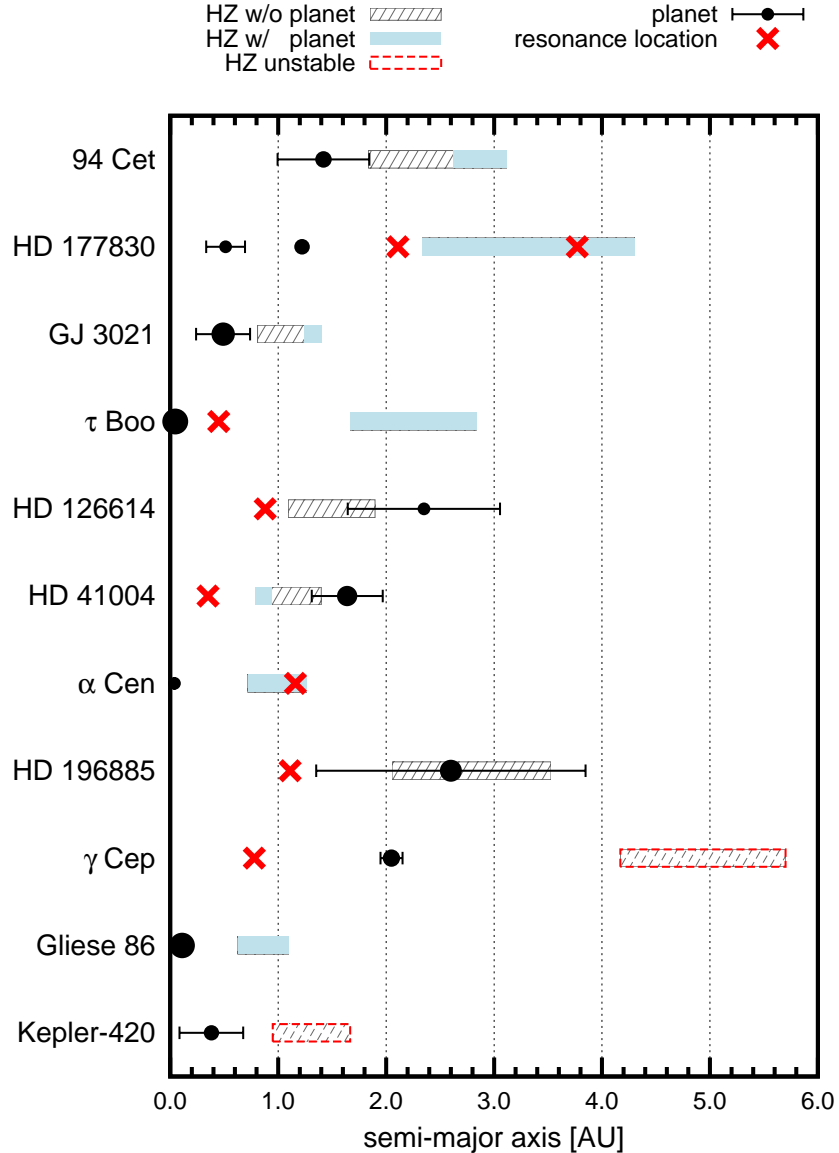


Fig. 2.— Habitable zones for the planet hosting star calculated without considering the giant planet (AHZ, hatched boxes), and with planetary perturbations (filled boxes). The two red-dashed regions are beyond the stability limit. Black dots with horizontal error bars show the position and eccentricity of the planet, while a red cross indicates the location of a secular resonance.

weak, because of the low eccentricity of the perturbing planet.

2.3. Notes on Individual Systems

In the following we briefly describe each system and collect the most important facts from the literature.

94 Ceti (HD 19994)

Mayor et al. (2004) announced a planet candidate in this system detected by radial-velocity measurements. The host star has a companion at a minimum separation of at least 100 AU, and we have adopted this minimum value for our study. This companion was first assumed to be an M-dwarf by Mayor et al. (2004), but Roell et al. (2012) argued that the companion is a close binary with a total mass of $0.9 M_{\odot}$. In our study we treat this binary companion as a single body; the difference in their actual spectral types does not play a significant role for calculating the habitable zone, because of the large distance to the planet.

HD 177830

This system is a special case among the ones selected for this study as it hosts two planets. The first planet (HD 177830 Ab) was announced by Vogt et al. (2000) based on data from a radial velocity survey, the second planet candidate (HD 177830 Ac) was presented by Meschiari et al. (2011) and is actually the inner planet of the two. An M-dwarf companion at a separation of 97 AU was reported in Eggenberger et al. (2007). The host star is an evolved star of spectral type K0IV (Meschiari et al. 2011), which has an impact

on the location of the habitable zone.

GJ 3021 (HD 1237)

The planet of GJ 3021 was announced by Naef et al. (2001), it was found with the radial velocity technique. Mugrauer et al. (2007) and Chauvin et al. (2007) found a long-period M-dwarf companion by follow-up observations with adaptive optics imaging and spectroscopy.

τ Bootis (HD 120136)

Butler et al. (1997) reported on the planetary companion of τ Boo, which is a hot-Jupiter type object with < 4 days orbital period. Eggenberger et al. (2004) attributed to this star a companion with a semi-major axis of 240 AU, while in Raghavan et al. (2006) the (projected) separation is given as 45 AU. This difference could be the result of a large eccentricity for the secondary star that is close to periastron passage (Roberts et al. 2011).

HD 126614

A long-term survey revealed that HD 126614 is a binary star system with a single giant planet (Howard et al. 2010). The presence of the stellar companion was proposed to account for a linear trend in the radial-velocity; a direct observation with adaptive optics revealed the true nature of the system. As the secondary star was not known before, some of its orbital parameters are not well constrained, especially the eccentricity is uncertain and just limited by $e_B < 0.6$. We used a value of $e_B = 0.5$ in our investigations, but the planet is located in the stable zone anyway. It is possible that there is a third star gravitationally

bound to this system in a much wider orbit (> 1000 AU).

α Centauri (HD 128621)

The α Centauri system consists of a close binary (α Cen A+B) and the M-dwarf Proxima Centauri separated by $> 10\,000$ AU (Endl et al. 2015). Dumusque et al. (2012) first claimed the discovery of a close-in planet with a few Earth masses in the α Centauri system. However, Hatzes (2013) cautioned that the radial velocity signal may be induced by stellar activity rather than a planet; recently Rajpaul et al. (2016) presented evidence for a false positive detection. Independent from the physical presence of the planet Eggl et al. (2013) and Andrade-Ines & Michtchenko (2014) investigated the stability of terrestrial planets in the habitable zone of the α Centauri binary. Both studies concluded that with a high probability additional planets can be present without inducing strong mutual perturbations with α Cen Bb.

HD 41004

HD 41004 consists of a K-type primary star and an M-type secondary star (Zucker et al. 2004), both stars have sub-stellar companions. The giant planet around HD 41004 A is listed in Table 1; HD 41004 B has a close-in brown dwarf companion with a minimum mass of 18 Jupiter masses in a 1.3 day orbit. In our investigation we have considered the HD 41004 B sub-system to be merged into a single object with the combined masses of the two bodies. This system and its HZ have been investigated extensively in Pilat-Lohinger & Funk (2010); Funk et al. (2015) and in EPL16. The semi-analytical method presented in section 3 was developed to explain numerical results obtained in those studies.

HD 196885

Correia et al. (2008) first announced a planet around the star HD 196885 A. They noted the presence of a stellar companion HD 196885 B, but they could only give constraints on its orbit. Chauvin et al. (2011) established the binary star nature of the two objects and presented updated orbital elements from a combined astrometric and radial velocity study for both the companion star and the planet. The inclination of the planet is still unknown, which motivated Giuppone et al. (2012) to perform a dynamical analysis of this system. Their results indicated that the giant planet is either nearly coplanar to the binary star’s orbital planet, or conversely it must have a high inclination prograde ($i = 44$ deg, or $i = 137$ deg retrograde) orbit. In the following we will assume a coplanar configuration for this system. However, note that both the giant planet and the secondary star have rather high eccentricities (see Figure 1), and at apoastron the planet approaches very closely the stability limit of this system (cf. Table 2).

γ Cephei (HD 222404)

γ Cephei was one of the first exoplanet candidates (Campbell et al. 1988). The nature of the signal was disputed until Hatzes et al. (2003) convincingly demonstrated that it is indeed a planet. Neuhäuser et al. (2007) provided a new orbital solution and an update of the system parameters (e.g. semi-major axis and eccentricity), that were slightly different before. The host star is an evolved K1III giant, which pushes the habitable zone quite far away from the star. The dynamics of this system was studied by Dvorak et al. (2003); Pilat-Lohinger (2005); Haghighipour (2006); Giuppone et al. (2011), and Funk et al. (2015), among others.

Gliese 86 (HD 13445)

The planet of Gliese 86 was discovered by Queloz et al. (2000) following a radial velocity measurement campaign. It was then already evident that the host star must posses another massive companion, which was characterised as a white dwarf by Mugrauer & Neuhäuser (2005) and Lagrange et al. (2006), while Fuhrmann et al. (2014) further constrained the parameters of this system. The HZ and dynamical stability of planets in this binary were investigated previously in Pilat-Lohinger & Funk (2010); Funk et al. (2015).

Kepler-420 (KOI-1257)

The *Kepler* space-telescope planetary candidate KOI-1257 was found via transit photometry and then confirmed by follow-up radial velocity observations (Santerne et al. 2014). Due to the combination of both methods this tight binary system is rather well characterised. However, the objects in this system exhibit large eccentricities (see Figure 1) such that the presence of additional planets interior or exterior to the orbit of the discovered one seems unlikely.

3. THE METHOD

To investigate the secular dynamics of the binary star systems we use a semi-analytical method, that combines the Laplace-Lagrange perturbation theory with a characteristic frequency determination derived from a single N -body numerical integration. This method is presented and discussed in more detail in EPL16, here we give just a quick summary.

3.1. Laplace-Lagrange Theory

The Laplace-Lagrange secular perturbation theory (LL) was developed to serve as a first approximation to the dynamical behaviour of the solar system (see Murray & Dermott 1999). It is a first order theory in the masses, and includes terms in the eccentricity and inclination of degree e^2 and $(\sin i)^2$, while higher order terms are neglected. Nevertheless, this approximation already allows to determine the location of the most important linear secular resonances.

Let us consider an exoplanetary system consisting of a test particle (of negligible mass) moving under the influence of the host star (m_0), a giant planet (m_1), and the secondary star (m_2). All bodies are assumed to be point mass objects and located in a common plane.

To set up the equations of motion usually the variables ($h = e \sin \varpi$, $k = e \cos \varpi$) are defined. The general solution to the equations of motion for this test particle is then of the form

$$h(t) = e_{\text{free}} \sin(gt + \phi) - \sum_{j=1}^2 \frac{\nu_j}{g - g_j} \sin(g_j t + \phi_j), \quad (1)$$

with a similar expression for $k(t)$. Here a , e , n , ϖ are the semi-major axis, eccentricity, mean motion, and longitude of pericenter of the test particle, respectively, and variables with subscript j are associated to the perturbers ($j = 1$ the giant planet, $j = 2$ the secondary star). The constants e_{free} and ϕ are given by the initial conditions for the particle, while g_j , ϕ_j , and ν_j follow from the secular dynamics of the massive perturbers.

The quantity g is the test particle's proper secular frequency calculated from

$$g = \frac{n}{4} \sum_{j=1}^2 \frac{m_j}{m_0} \alpha_j \bar{\alpha}_j b_{3/2}^{(1)}(\alpha_j). \quad (2)$$

This frequency g depends on the semi-major axes of the particle and of the perturbers via the ratio $\alpha_j = a/a_j$ (in case $a < a_j$) or $\alpha_j = a_j/a$ (when $a > a_j$), the Laplace coefficient $b_{3/2}^{(1)}(\alpha_j)$, as well as on the perturber's mass m_j .

Wherever $g \approx g_j$ in equation (1), the particle’s secular frequency equals one of the perturber’s frequencies, which then gives rise to a secular resonance. In these cases the particle suffers from large secular perturbations due to the perturber j , where the particle’s forced eccentricity can reach values close to $e = 1$. Then, it can cross the orbit of the giant planet or be ejected from the system by a close approach to the host star.

3.2. Numerical Part of the Application

In equation (1) we need to know the frequencies g_j accurately in order to determine the location where $g - g_j \approx 0$, i.e. the location of a linear secular resonance. We chose to determine the fundamental frequencies numerically throughout this study. This is necessary as the eccentricities of the binary stars are considerable ($e_B \geq 0.2$, see Table 1) for all selected systems, such that a low-order analytical theory (like the LL theory) has only a limited accuracy.

We used the Lie-series method (Hanslmeier & Dvorak 1984; Eggl & Dvorak 2010; Bancelin et al. 2012) and the Mercury integrator’s Radau method (Chambers 1999; Everhart 1974) as complementary tools to integrate the equations of motions of the selected binary star-planet system. Although one single numerical simulation of the respective system suffices to estimate the dominant frequencies, it must be long enough to cover several secular periods of the giant planet (typically $\lesssim 10^7$ years). Fortunately it is not necessary to cover a whole secular period for secondary stars on wide orbits, because their periods will be rather large—typically 10^8 years and longer—due to the comparatively small mass of the perturbing planet and the small ratio a_P/a_B . For closer binary systems with $a_B \leq 25$ AU the integration time generally need not be longer than several 10^6 years to cover multiple secular periods of the giant planet as well as a complete secular period of the secondary

star.¹ This first estimate for the secondary’s secular period is already accurate enough to state that it is vastly different (by orders of magnitude) from the periods of objects in the HZ; accordingly, we can assume that the secondary star will not cause important secular resonances in the region of interest.

We then performed a frequency analysis on the data to extract the fundamental frequencies; this step was accomplished by using the Fast-Fourier Transform (FFT) library FFTW² of Frigo & Johnson (2005). As an independent check we used the tool SigSpec of Reegen (2007), that performs a Discrete Fourier Transform (DFT) and gives the probability that a peak is not due to noise in the time-series. Whenever possible we removed short period contributions (associated with the orbital frequencies of the giant planet and the secondary star) by a low-pass filter. From the frequency analysis we obtain the giant planet’s secular frequency g_P (or g_1), which is effectively the averaged frequency $\langle g(t) \rangle_T$ over the integration time T . On a still longer time-scale the gravitational influence of the secondary star can modify this value.

Finally, to determine the locations of secular resonances for the test particles we identified the intersection points of equation (2) with the values g_j .

3.3. Relativistic Effects

From Table 1 we can observe that there are several planets with $a_P \lesssim 0.5$ AU. For such planets the general relativistic precession of the perihelion becomes important, like in the case of Mercury in our solar system (Laskar 2008). This additional precession frequency is

¹ $g_B \lesssim 5 \times 10^6$ years for HD 41004, HD 196885, and γ Cep, except for close-in planets like Gliese 86.

²<http://fftw.org/>

most important for very close-in planets, such that we chose to include it in the simplified form of Brasser et al. (2009) (see also Beutler 2005). We do not include tidal effects between the close-in planets and the host star (see Fabrycky & Tremaine 2007), because the orbits are already quite circular, such that a further circularisation is not expected.

Figure 3 demonstrates that the general relativistic precession can be orders of magnitude larger than the precession frequency induced by the purely Newtonian interaction between the giant planet and secondary star. For the three systems τ Boo, α Cen, and Gliese 86 we have to consider this additional contribution.

4. RESULTS

We applied the semi-analytical method to all candidates in Table 1. Additionally, we investigated some systems in more detail by numerical integrations, in order to check the accuracy of the results. These test calculations involve test particles that cover a range of semi-major axes around the location of the major secular resonance.

4.1. Interior vs Exterior Planets

We find a qualitative difference in the dynamics of (massless) test planets depending on the location of the giant planet. When the giant planet is exterior to the orbit of the test planets (we refer to these as “exterior cases”), i.e. $a < a_P$ like Jupiter in the solar system, generally secular resonances appear in the region of interest. Contrary to this, for interior giant planets (“interior cases”) with $a_P < a$ no such resonance occur, except for the HD 177830 system. The explanation for this result lies in the behaviour of the analytical curve described by equation (2). In the exterior case the periods for the test planets decrease monotonically from a large value nearby the host star and approach zero

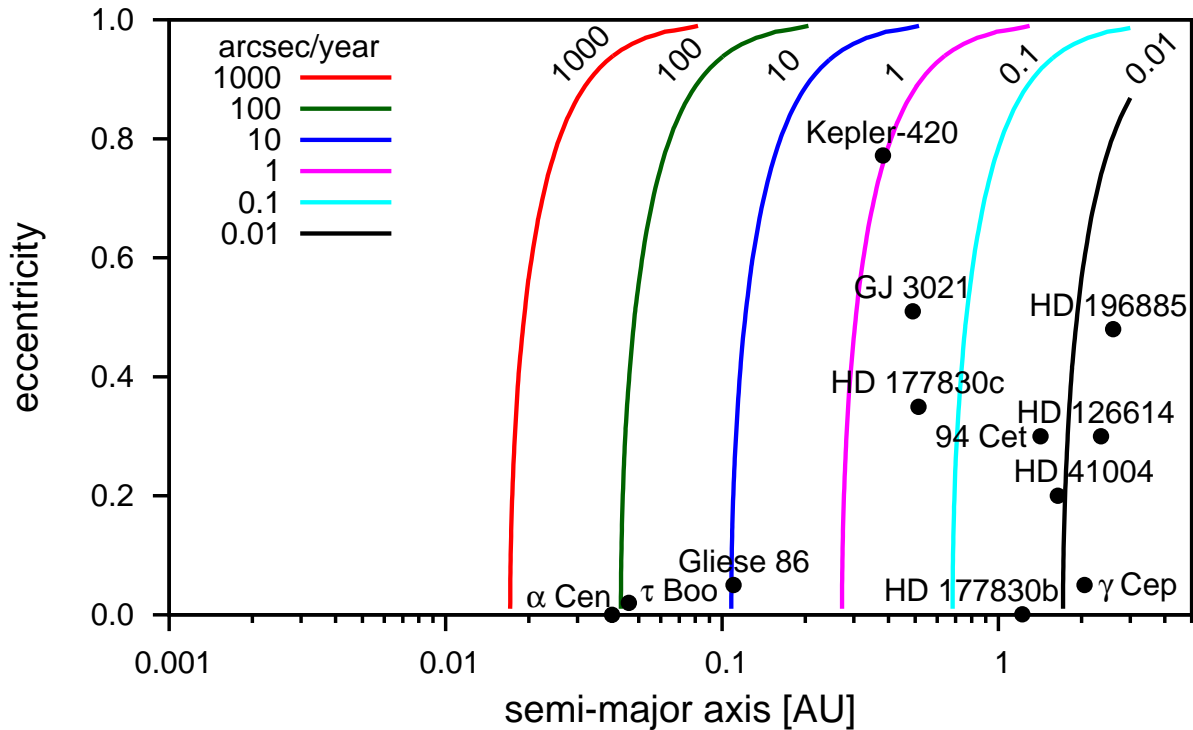


Fig. 3.— Order of magnitude estimate of the general relativistic precession of perihelion (in arcseconds per year) for different binary star systems. The planets are plotted according to the main parameters semi-major axis and eccentricity; the host star’s mass is implicitly included. The contour lines indicate the different magnitudes of the general relativistic precession.

as $a \rightarrow a_P$ (because of the properties of the Laplace coefficient $b_{3/2}^{(1)}(\alpha)$ when $\alpha \rightarrow 1$). For the interior case the periods are first low in the vicinity of the giant planet, but then rise to some peak value before they start decreasing again under the influence of the secondary star (see Figure 4). The interior giant planet tends to have such a large secular period that the test planet’s proper period cannot reach the same value. In our sample the secular periods of the giant and the test planets are differing by more than a factor of ten. Consequently, interior giant planets—like GJ 3021 or Gliese 86—are unable to cause a linear secular resonance, while giant planets exterior to the terrestrial planet are capable of doing so.

Figure 4 displays plots of the test planet’s proper secular period depending on the planet’s semi-major axis. The intervals are chosen in such a way, that the test particles never approach the giant planet closer than three Hill radii, or alternatively the pericenter (for column (a)) and apocenter (for the other two columns) distance of the giant planet, whichever is larger.

The systems in the left column all belong to the exterior giant planet type, and consequently exhibit a resonance; three of them will be discussed in the following section. The systems in the central column of the figure belong to the interior giant planet type and show no sign of a linear secular resonance. As mentioned above, HD 177830 is an exception, because there are two giant planets (at ~ 0.5 and ~ 1.2 AU) that perturb each other. This mutual gravitational interaction increases the apsidal precession frequencies relative to those that would be caused by the secondary star alone. The corresponding giant-planet secular periods are $< 10^5$ years in the four-body problem, instead of $> 10^6$ years in the three-body case otherwise. For Gliese 86, τ Boo, and α Cen in the right column we have added the effect of the general relativistic precession, which makes a difference for the latter two. These close-in planets would have much too large apsidal periods to cause a resonance, but by adding the GR effect we can observe that in principle a resonance will

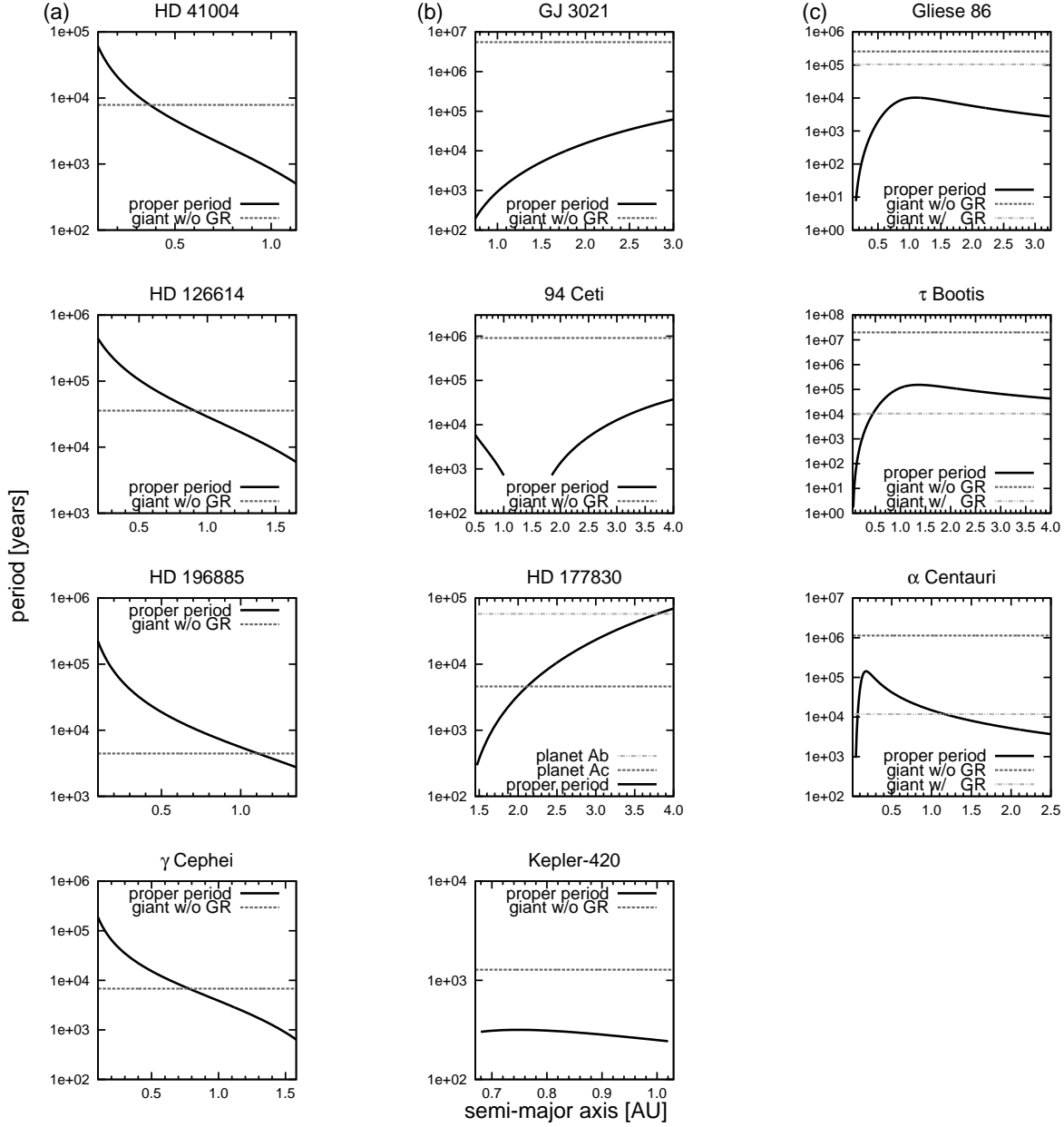


Fig. 4.— Plot of the proper secular periods of test planets as a function of their semi-major axis. An intersection of the black curve with the horizontal line indicates the occurrence of a linear secular resonance. The left column (a) collects systems with exterior giant planets, the central column (b) shows systems with a giant planet that is interior to the orbit of the test planet, while the right column (c) presents those cases where the close-in giant planet is affected by the general relativistic precession (dashed line without GR, dot-dashed line including GR).

occur. However, due to the planet’s small eccentricities their perturbing effect will be weak; additionally α Cen Bb has a small mass. The plot for α Cen shows two intersection points, in Table 2 we have only included the more distant resonance location that is closer to the HZ.

4.2. Application to Example Systems

Next we perform an in-depth investigation of the systems in the left column of Figure 4, where a linear secular resonance is present. HD 41004 is investigated separately in EPL16.

HD 196885

In this system the giant planet occupies the habitable zone entirely, cf. Tables 1 & 2 and Figure 2. The planet reaches a distance of ≈ 1.3 AU from the host star in the pericenter because of its large eccentricity, while the inner border of the HZ is at about 2 AU.

In Figure 5 we plot the maximum eccentricities of test particles reached over an integration time of 10^6 years in the top part. For this simulation we reduced the giant planet’s initial eccentricity to $e_P = 0.3$ in order to assess the influence of this parameter on the test particles’ maximum eccentricity. All test particles start on initially circular orbits, but those beyond $a \simeq 0.9$ AU quickly reach a value of $e \geq 1$ and are ejected from the system by a close encounter with the giant planet. For two other initial conditions we observe a local increase of the maximum eccentricity. These locations correspond to the non-linear secular resonances $2g - g_P = 0$ and $3g - g_P = 0$, while nearby there are also the 6:1 and 8:1 mean motion resonances at $a \approx 0.79$ and $a \approx 0.65$ AU, respectively. In the bottom part of the figure we show the intersection points of the test particle’s proper secular period curve (dashed black) with multiples of the giant planet’s period (P_{GP} ; the horizontal lines).

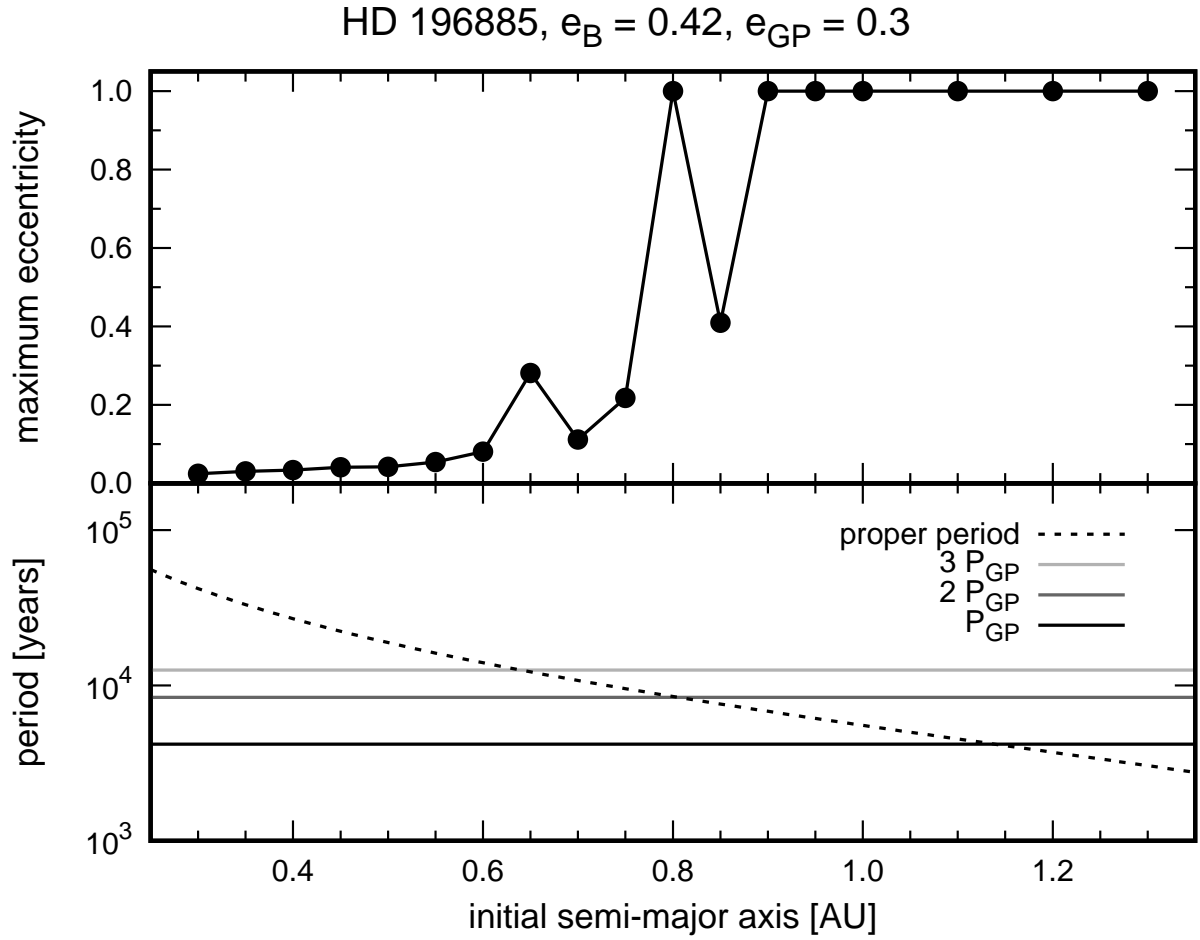


Fig. 5.— Effect of the secular resonance on test particles in the HD 196885 system in case of $e_P = 0.3$. Over a time interval of $T = 10^6$ years the maximum eccentricity rises to unity (top) at the locations where the test particle's proper period (bottom; dashed black curve) is equal to multiples of the giant planet's secular period (horizontal lines).

We can conclude that the region investigated in Figure 5 is destabilised by the secular increase of the test particle’s eccentricity leading to close encounters with the giant planet. We do not expect to find any additional planets in this system with semi-major axes larger than $a = 0.6$ given that the giant planet actually has an even higher eccentricity. Any planet closer to the host star than this threshold would have too high surface temperatures—the star is of spectral type F8 V (Correia et al. 2008)—and thus would not be habitable.

γ Cephei

In the γ Cep system a giant planet orbits the host star of spectral type K1 III (Hatzes et al. 2003) in a distance of about 2 AU. The current orbital solution of Endl et al. (2011) gives an eccentricity of $e_P = 0.049 \pm 0.034$ for the giant planet, whereas in the original Hatzes et al. (2003) solution the eccentricity was $e_P = 0.12$. For an investigation of the dynamics with the latter parameters see Dvorak et al. (2003); Pilat-Lohinger (2005), while e.g. Funk et al. (2015) investigated the dynamics for the lower value. The newer value for the eccentricity is actually close to the dynamically relaxed value of $e_F \approx 0.056$ for the forced eccentricity obtained by Andrade-Ines et al. (2016) from an analytical model.

The host star’s current evolutionary state has shifted the habitable zone for this system beyond the stability limit (cf. Table 2). Therefore we can assume that during the main-sequence period of the host star the region around $a \approx 1$ AU has never been perturbed by a highly eccentric giant, and could have harboured habitable planets. We will investigate this region in more detail now, but note that this was probably the inner border of the HZ.

From a dynamical point of view the situation is similar to the HD 196885 system, the giant planet causes a secular resonance in the region around $a = 1$ AU, although the planet’s eccentricity is much lower here. Figure 6 shows the variation of maximum

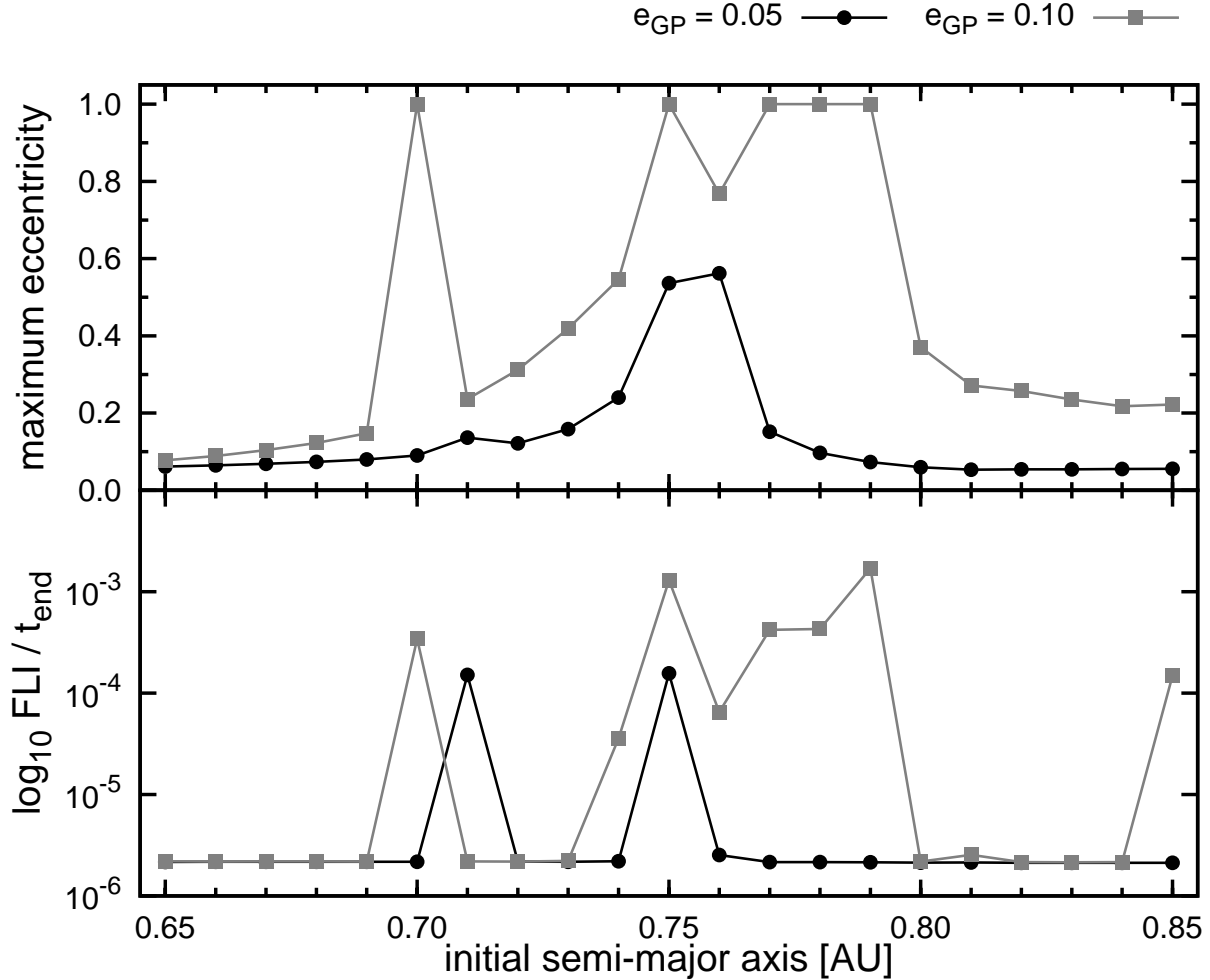


Fig. 6.— Effect of the secular resonance on test particles in the γ Cephei system for two values of the giant planet's eccentricity (black and grey curves). Top: The maximum eccentricity as a function of the initial semi-major axis. Bottom: normalised FLI of the same region.

eccentricity (top) and Fast Lyapunov Indicator (FLI; bottom) as a function of the initial semi-major axis of test particles. In the first case for $e_P = 0.05$ (black curve) there is a peak in the eccentricity distribution around $a = 0.76$ AU and a smaller peak at $a = 0.71$ AU, these peaks correspond to the 9:2 and 5:1 mean-motion resonances, respectively. The FLI is a chaos indicator that is sensitive to mean-motion resonances (Froeschlé et al. 1997); it clearly indicates the two MMR (black curve in the bottom part of Figure 6). A low FLI value means regular motion, while a high value indicates chaotic motion. Although the 9:2 MMR and the secular perturbation overlap partly, even their joint effect does not raise the maximum eccentricity above $e = 0.5$. Increasing the giant planet’s eccentricity to $e_P = 0.1$ has a strong effect on the test particles (grey curves). The maximum eccentricities now reach values sufficient for ejection from the system. This is demonstrated by the two narrow peaks at the locations of the two MMR mentioned above, and by the flat plateau due to the secular resonance; the effect is also visible in the FLI results (bottom).

The main mechanism responsible for the strong increase of the maximum eccentricities is the forced eccentricity component, which depends on the perturber’s eccentricity. A minor increase in the giant planet’s eccentricity from 0.05 to 0.1 is sufficient to drive the forced eccentricity to values near unity, i.e. already a slightly eccentric giant planet is able to perturb planets quite effectively. The overlap of (relatively high-order) MMR and SR (Wisdom 1980) clearly leads to chaotic behaviour and effectively empties the region around the SR.

HD 126614

The HD 126614 system is another typical representative of the exterior giant planet case. The secondary star’s eccentricity is unknown, only an upper bound $e_B < 0.6$ is given. This uncertainty influences to a certain degree the location of the secular resonance, which

shifts to lower semi-major axes as e_B shrinks.

While the planet grazes the outer part of the habitable zone in pericenter, its eccentricity of $e = 0.3$ leads to unstable test particle orbits everywhere in the HZ. Although the location of the secular resonance would be situated outside the inner border of the HZ (cf. Table 2), several mean-motion resonances appear right inside the HZ, among others the low order 3:1 and 2:1 MMR.

5. DISCUSSION

The semi-analytical method presented in section 3 relies on a numerical integration of the equations of motion to extract the fundamental frequencies of the system. This number is then fed into the analytical model to calculate the secular frequencies of test planets. An analytical approach involving simple expressions for the perturber’s frequency would facilitate the study of a wide variety of systems, including newly detected ones.

5.1. Purely Analytical Methods

There are various analytical methods to calculate the fundamental frequencies g_j , including the Laplace-Lagrange secular theory (Murray & Dermott 1999), the methods of Heppenheimer (1978) and of Giuppone et al. (2011).

The Laplace-Lagrange theory (LL) can be used to calculate the secular frequencies of an arbitrary number N of mutually interacting massive bodies. If the assumptions of low eccentricity and inclination are fulfilled, the frequencies are obtained as the eigenvalues of a quadratic $N \times N$ matrix (see Murray & Dermott 1999, section 7).

In the Heppenheimer (1978) model (HEP) a restricted three-body problem is assumed,

where the planet’s mass is negligible relative to the masses of the two stars. The disturbing function is limited to terms of $\mathcal{O}(e_P^2)$ in the planet’s eccentricity, but it can handle an arbitrary eccentricity e_B of the binary (see Andrade-Ines et al. 2016). The expression for the forced secular frequency of the giant planet is

$$g_P = \frac{3}{4} \left(\frac{m_B}{m_A} \right) \left(\frac{a_P}{a_B} \right)^3 n_P (1 - e_B^2)^{-3/2}, \quad (3)$$

where n_P is the giant planet’s mean motion.

Giuppone et al. (2011) constructed a secular model (GIU) building on the Heppenheimer model, but extending it to second order in the masses. This means that it also assumes a restricted three-body problem, and hence cannot be applied in case of more than one perturbing planet (besides the secondary star). Although the authors demonstrate that their model leads to considerable improvements, they also state that the model was too complicated for practical use. Instead, they constructed an empirical model for the frequency by fitting a simple formula to their second-order model, which is given by

$$g_P = g_0 \left[1 + 32 \left(\frac{m_B}{m_A} \right) \left(\frac{a_P}{a_B} \right)^2 (1 - e_B^2)^{-5} \right], \quad (4)$$

where g_0 is given by the expression in equation (3). Strictly speaking, their formula was fitted to the γ Cep system, and was not intended to be used elsewhere.

In Figure 7 we use these three analytical methods (LL, HEP, GIU) to calculate the secular frequency of the giant planet, and compare their errors relative to the reference value obtained from a numerical simulation (without relativity). In the HD 177830 system there are four massive bodies instead of three as presumed by the HEP and GIU models; owing to this inherent inability we do not show HD 177830 in that figure. It is obvious that in some cases the analytical frequencies are off by a large amount, while in other cases they are quite reliable. For instance, the relative errors of the latter two methods are below the 1 % level for the 94 Cet system. The LL method shows the largest overall errors, which

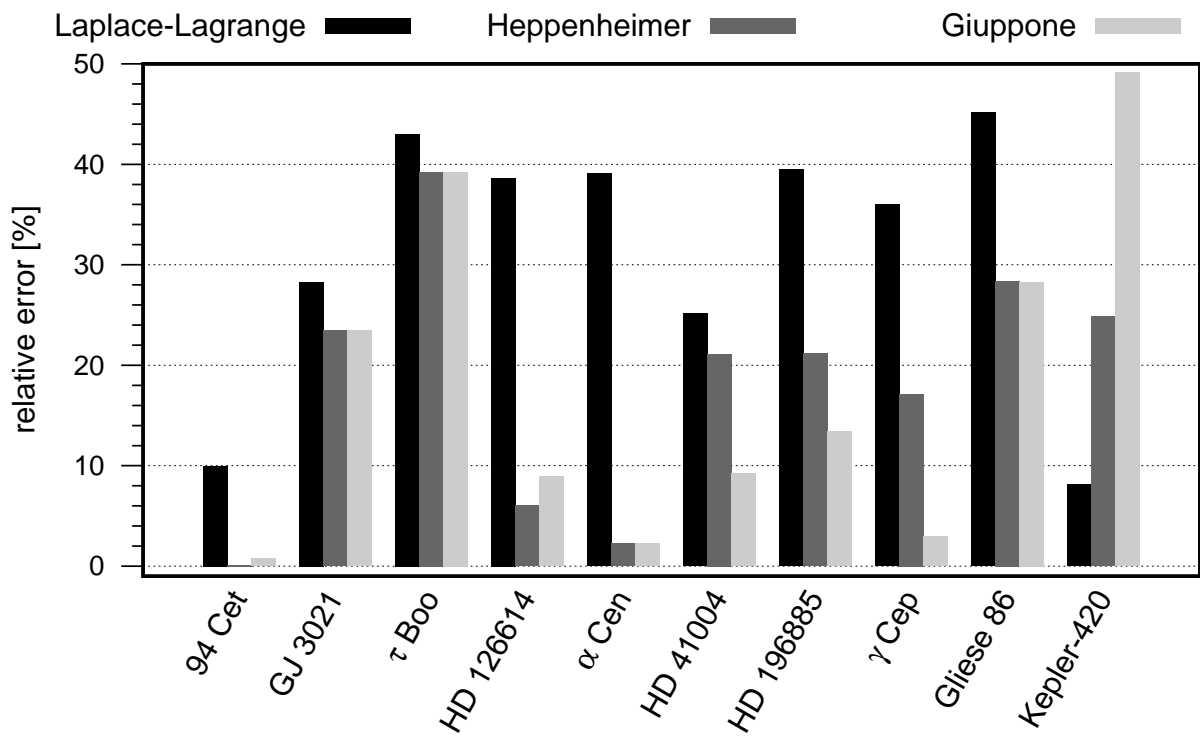


Fig. 7.— Magnitude of relative errors for different analytical methods used to determine the fundamental frequency of the giant planet. The reference value for the frequency is derived from a numerical integration. For HD 177830 the Heppenheimer and Giuppone methods are not applicable, see text for details.

is due to its construction of neglecting higher-order terms in the eccentricity. The one exception to this trend is the Kepler-420 case, here the LL performs best among the three methods. One reason for the mismatch in the analytical frequency for this particularly tight binary system is the combination of the semi-major axis ratio $\alpha = a_P/a_B$ (or orbital period ratio) with the mass of the secondary star. Comparing the HEP and GIU methods we see that they perform in a similar way. They agree fairly well in most cases; for the two systems HD 126614 and Kepler-420 the Heppenheimer method has an advantage, though. Nevertheless, when considering only the four interesting cases from column (a) of Figure 4, the GIU method performs better in three of them.

It is also instructive to compare equations (2), (3), and (4) when used to calculate the frequencies of test planets. Figure 8 plots the secular periods of test planets as a function of their semi-major axes for γ Cep. On the top axis the semi-major axis ratio α is shown, which is important as a small parameter in the HEP and GIU methods. For small values of α the curves agree fairly well, while for larger values they diverge. This behaviour can be understood when recalling that the LL method takes into account also the contribution from the secondary star, but more importantly the HEP and GIU methods are limited by the convergence rate of the Legendre expansions, see Andrade-Ines et al. (2016) for a discussion on this issue. When we include the giant planet period from the numerical integration (horizontal line), it becomes clear that these methods result in very different locations for the secular resonance.

Table 3 gives a comparison of the performance of the analytical methods for the exterior giant planet cases from Figure 4. The semi-analytical method serves as a reference (cf. locations in Table 2), where we used a combination of a numerical integration of the respective system for the giant planet frequency, and the LL model for the test planet frequency. All other entries are pairs of methods, where the first item identifies the

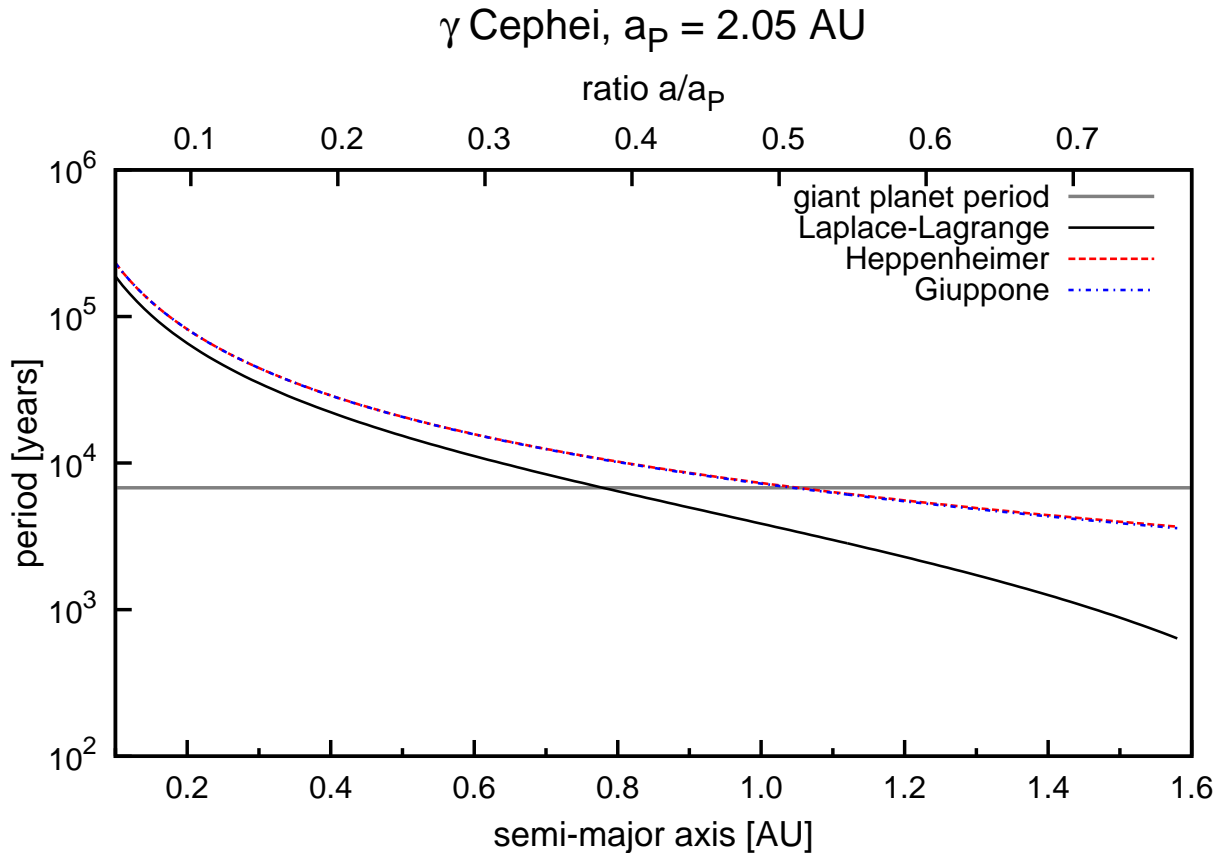


Fig. 8.— Comparison of the proper periods of test planets depending on their semi-major axis. The curves were calculated using the analytical methods of Laplace-Lagrange (solid black), Heppenheimer (dashed red), and Giuppone et al. (dot-dashed blue). The latter two curves are indiscernible in this plot. A grey horizontal line marks the time-averaged secular period of the giant planet located at 2.05 AU. Looking at the intersection points of the curves with that line it is well visible that these methods would predict quite different locations of the linear secular resonance.

Table 3: Comparing the location of the secular resonance obtained by combinations of different analytical methods with the reference semi-analytical method.

Method	Resonance Location (AU) for System			
	HD 41004	HD 126614	HD 196885	γ Cep
semi-analytical	0.37	0.91	1.11	0.78
LL/LL	0.30	0.70	0.87	0.62
HEP/HEP	0.32	0.98	1.06	0.93
HEP/LL	0.32	0.88	0.99	0.71
GIU/GIU	0.35	1.08	1.29	1.06
GIU/LL	0.35	0.94	1.17	0.79

Note. — For each pair the first item indicates the model to calculate the giant planet's frequency, the second item the model for the test planet frequency. Abbreviations: LL = Laplace-Lagrange, HEP = Heppenheimer, GIU = Giuppone.

model for the giant planet’s frequency, and the second item the model for the test planet frequencies. A crucial ingredient is the giant planet’s secular frequency g_P ; differences in this frequency (cf. Figure 7) transform into deviations Δa of several 0.1 AU in the location of the resonance. If we compare mixed pairs involving the LL method, we can see that usually they are closer to the numerical data—see maximum eccentricity plots in Figures 5 and 6—than pairs of purely one method. There might exist a correlation between the deviations in the location of the secular resonance and the eccentricity of the perturbed planet. However, more systems with more diverse parameters have to be analysed in order to quantify this correlation, or to disprove it.

5.2. More General Methods

The semi-analytical method can be supplemented also in another way. So far we have considered only coplanar systems, but the orbital inclination is another important parameter. Pilat-Lohinger et al. (2016) demonstrate for the HD 41004 system that the secular resonance can be traced numerically for inclinations up to $i \sim 40^\circ$.

Williams & Faulkner (1981) presented a method to map the secular resonance surfaces in the proper (a, e, i) space. They applied this method to the solar system and investigated the main linear secular resonances (with Jupiter and Saturn) in the asteroid main belt.

A drawback of using the simple Laplace-Lagrange model is that we need to assume that test particles start with negligible initial eccentricity (and inclination). Veras & Armitage (2007) worked out an improved Laplace-Lagrange theory by extending it to fourth order in the eccentricity. Although this generalised theory gives somewhat more accurate results than the traditional one, they conclude that its usefulness for extrasolar planetary systems is limited. The main point is that the fundamental secular frequencies are proportional

to the perturbed mass / host star mass ratio and the semi-major axis ratio α —just like equation (2) demonstrates for the proper frequency—but usually these quantities are much larger in extrasolar systems than in the “traditional” case for the solar system.

One possible way to circumvent these difficulties is to invoke second-order models (in the masses) to study such systems. In a series of papers, Georgakarakos (2003, 2009) worked out such a model for hierarchical triple systems, i.e. a close binary (or star-planet pair) with a much more distant third object. This setup would be well adaptable to our sample. He derived a closed formula for the eccentricity evolution of the inner object and its secular frequency. However, this model is valid only for three-body problems by construction; additionally the inner object should start with nearly zero eccentricity.

This path has also been followed by Giuppone et al. (2011), as mentioned above, and more recently by Andrade-Ines et al. (2016). The latter authors constructed a second-order model (in the masses) and determined the limits of its validity. The model complexity increased considerably as compared to the first order model, but they could show that for some of their investigated systems only the second order model was capable to correctly describe the dynamics. However, for a few extreme cases neither the first nor the second order model was sufficient, in those cases a direct numerical integration remains the only viable option.

Libert & Henrard (2005) used a similar approach with a high order expansion of the disturbing function in the eccentricities to cope with moderately to highly eccentric extrasolar systems. Libert & Sansottera (2013) extended the previous work by also moving to a second order theory with respect to the masses.

6. SUMMARY

We have studied 11 binary star systems with detected planets in circumstellar (S-type) motion. For these systems we calculated the location and extent of the habitable zone. Most planets are gas giants, with masses similar to that of Jupiter, moving outside the HZ. We investigated the dynamics of additional hypothetical planets inside or close to the HZ. The main goal was to detect whether a secular resonance with the giant planet affects the dynamical stability of the additional planets. We use a semi-analytical approach, that combines the Laplace-Lagrange secular theory to calculate the proper secular frequency for test planets, with a numerical integration of the equations of motion to derive the fundamental secular frequencies of the perturbing bodies. It is shown that, for giant planets located exterior to the HZ, there generally occurs a linear secular resonance; this affects four of the eleven systems. In the case of giant planets interior to the HZ we do not observe such a resonance, except for one multi-planetary system. However, for close-in giant planets ($a \leq 0.1$ AU) the general relativistic precession of the pericenter introduces another source that can contribute to a secular resonance, this happens for another two systems. We compared the accuracy of our semi-analytical method to three analytical theories, showing that the most accurate results are still obtained from the numerical integration.

The authors acknowledge support by FWF projects S11608-N16 and P22603-N16. For this investigation we made use of the Extrasolar Planet Encyclopaedia³ maintained by J. Schneider, and the Binary Catalogue of Exoplanets⁴ maintained by R. Schwarz.

³<http://exoplanet.eu>

⁴<http://www.univie.ac.at/adg/schwarz/multiple.html>

REFERENCES

Andrade-Ines, E., Beaugé, C., Michtchenko, T., & Robutel, P. 2016, CMDA, 124, 405

Andrade-Ines, E., & Michtchenko, T. A. 2014, MNRAS, 444, 2167

Armstrong, D. J., Osborn, H. P., Brown, D. J. A., et al. 2014, MNRAS, 444, 1873

Bancelin, D., Hestroffer, D., & Thuillot, W. 2012, CMDA, 112, 221

Barclay, T., Quintana, E. V., Adams, F. C., et al. 2015, ApJ, 809, 7

Beaugé, C., Ferraz-Mello, S., & Michtchenko, T. A. 2012, Research in Astronomy and Astrophysics, 12, 1044

Beaugé, C., & Nesvorný, D. 2012, ApJ, 751, 119

Beutler, G. 2005, Methods of celestial mechanics. Vol. I: Physical, mathematical, and numerical principles, Astronomy and Astrophysics Library (Springer, Berlin)

Boss, A. P. 2006, ApJ, 641, 1148

Brasser, R., Morbidelli, A., Gomes, R., Tsiganis, K., & Levison, H. F. 2009, A&A, 507, 1053

Bromley, B. C., & Kenyon, S. J. 2015, ApJ, 806, 98

Butler, R. P., Marcy, G. W., Williams, E., Hauser, H., & Shirts, P. 1997, ApJL, 474, L115

Campbell, B., Walker, G. A. H., & Yang, S. 1988, ApJ, 331, 902

Chambers, J. E. 1999, MNRAS, 304, 793

Chauvin, G., Beust, H., Lagrange, A.-M., & Eggenberger, A. 2011, A&A, 528, A8

Chauvin, G., Lagrange, A.-M., Udry, S., & Mayor, M. 2007, A&A, 475, 723

Correia, A. C. M., Udry, S., Mayor, M., et al. 2008, *A&A*, 479, 271

Cuntz, M. 2014, *ApJ*, 780, 14

Dodson-Robinson, S. E., Veras, D., Ford, E. B., & Beichman, C. A. 2009, *ApJ*, 707, 79

Dumusque, X., Pepe, F., Lovis, C., et al. 2012, *Nature*, 491, 207

Duquennoy, A., & Mayor, M. 1991, *A&A*, 248, 485

Dvorak, R., Froeschle, C., & Froeschle, C. 1989, *A&A*, 226, 335

Dvorak, R., Pilat-Lohinger, E., Funk, B., & Freistetter, F. 2003, *A&A*, 398, L1

Eggenberger, A., Udry, S., Chauvin, G., et al. 2007, *A&A*, 474, 273

Eggenberger, A., Udry, S., & Mayor, M. 2004, *A&A*, 417, 353

Eggl, S., & Dvorak, R. 2010, in *Lecture Notes in Physics*, Berlin Springer Verlag, Vol. 790, *Lecture Notes in Physics*, Berlin Springer Verlag, ed. J. Souchay & R. Dvorak, 431–480

Eggl, S., Haghjipour, N., & Pilat-Lohinger, E. 2013, *ApJ*, 764, 130

Eggl, S., Pilat-Lohinger, E., Georgakarakos, N., Gyergyovits, M., & Funk, B. 2012, *ApJ*, 752, 74

Endl, M., Cochran, W. D., Hatzes, A. P., & Wittenmyer, R. A. 2011, in *American Institute of Physics Conference Series*, Vol. 1331, *American Institute of Physics Conference Series*, ed. S. Schuh, H. Drechsel, & U. Heber, 88–94

Endl, M., Bergmann, C., Hearnshaw, J., et al. 2015, *International Journal of Astrobiology*, 14, 305

Everhart, E. 1974, *Cel. Mech.*, 10, 35

Fabrycky, D., & Tremaine, S. 2007, *ApJ*, 669, 1298

Frigo, M., & Johnson, S. G. 2005, *Proceedings of the IEEE*, 93, 216, special issue on “Program Generation, Optimization, and Platform Adaptation”

Froeschlé, C., Lega, E., & Gonczi, R. 1997, *CMDA*, 67, 41

Fuhrmann, K., Chini, R., Buda, L.-S., & Pozo Nuñez, F. 2014, *ApJ*, 785, 68

Funk, B., Pilat-Lohinger, E., & Eggl, S. 2015, *MNRAS*, 448, 3797

Georgakarakos, N. 2003, *MNRAS*, 345, 340

—. 2009, *MNRAS*, 392, 1253

Giuppone, C. A., Leiva, A. M., Correa-Otto, J., & Beaugé, C. 2011, *A&A*, 530, A103

Giuppone, C. A., Morais, M. H. M., Boué, G., & Correia, A. C. M. 2012, *A&A*, 541, A151

Gould, A., Udalski, A., Shin, I.-G., et al. 2014, *Science*, 345, 46

Haghighipour, N. 2006, *ApJ*, 644, 543

Hanslmeier, A., & Dvorak, R. 1984, *A&A*, 132, 203

Hatzen, A. P. 2013, *ApJ*, 770, 133

Hatzen, A. P., Cochran, W. D., Endl, M., et al. 2003, *ApJ*, 599, 1383

Heppenheimer, T. A. 1978, *A&A*, 65, 421

Holman, M. J., & Wiegert, P. A. 1999, *AJ*, 117, 621

Howard, A. W., Johnson, J. A., Marcy, G. W., et al. 2010, *ApJ*, 721, 1467

Jaime, L. G., Aguilar, L., & Pichardo, B. 2014, *MNRAS*, 443, 260

Jang-Condell, H. 2015, *ApJ*, 799, 147

Kaltenegger, L., & Haghishipour, N. 2013, *ApJ*, 777, 165

Kasting, J. F., Whitmire, D. P., & Reynolds, R. T. 1993, *Icarus*, 101, 108

Kley, W., & Nelson, R. P. 2010, in *Astrophysics and Space Science Library*, Vol. 366, Planets in Binary Star Systems, ed. N. Haghishipour, 135

Kopparapu, R. K., Ramirez, R., Kasting, J. F., et al. 2013, *ApJ*, 765, 131

Lagrange, A.-M., Beust, H., Udry, S., Chauvin, G., & Mayor, M. 2006, *A&A*, 459, 955

Laskar, J. 2008, *Icarus*, 196, 1

Libert, A.-S., & Henrard, J. 2005, *CMDA*, 93, 187

Libert, A.-S., & Sansottera, M. 2013, *CMDA*, 117, 149

Marois, C., Macintosh, B., Barman, T., et al. 2008, *Science*, 322, 1348

Mayor, M., Udry, S., Naef, D., et al. 2004, *A&A*, 415, 391

Meschiari, S., Laughlin, G., Vogt, S. S., et al. 2011, *ApJ*, 727, 117

Mugrauer, M., & Neuhäuser, R. 2005, *MNRAS*, 361, L15

—. 2009, *A&A*, 494, 373

Mugrauer, M., Neuhäuser, R., & Mazeh, T. 2007, *A&A*, 469, 755

Murray, C. D., & Dermott, S. F. 1999, *Solar system dynamics* (Cambridge University Press)

Naef, D., Mayor, M., Pepe, F., et al. 2001, *A&A*, 375, 205

Naoz, S., Farr, W. M., & Rasio, F. A. 2012, *ApJL*, 754, L36

Neuhäuser, R., Mugrauer, M., Fukagawa, M., Torres, G., & Schmidt, T. 2007, *A&A*, 462, 777

Pilat-Lohinger, E. 2005, in IAU Colloq. 197: Dynamics of Populations of Planetary Systems, ed. Z. Knežević & A. Milani, 71–76

Pilat-Lohinger, E., Bazsó, Á., & Funk, B. 2016, submitted to *ApJ*

Pilat-Lohinger, E., & Dvorak, R. 2002, *CMDA*, 82, 143

Pilat-Lohinger, E., & Funk, B. 2010, in Lecture Notes in Physics, Berlin Springer Verlag, Vol. 790, Lecture Notes in Physics, Berlin Springer Verlag, ed. J. Souchay & R. Dvorak, 481–510

Poleski, R., Skowron, J., Udalski, A., et al. 2014, *ApJ*, 795, 42

Queloz, D., Mayor, M., Weber, L., et al. 2000, *A&A*, 354, 99

Quintana, E. V., Adams, F. C., Lissauer, J. J., & Chambers, J. E. 2007, *ApJ*, 660, 807

Rabl, G., & Dvorak, R. 1988, *A&A*, 191, 385

Raghavan, D., Henry, T. J., Mason, B. D., et al. 2006, *ApJ*, 646, 523

Raghavan, D., McAlister, H. A., Henry, T. J., et al. 2010, *ApJS*, 190, 1

Rajpaul, V., Aigrain, S., & Roberts, S. 2016, *MNRAS*, 456, L6

Reegen, P. 2007, *A&A*, 467, 1353

Roberts, Jr., L. C., Turner, N. H., ten Brummelaar, T. A., Mason, B. D., & Hartkopf, W. I. 2011, *AJ*, 142, 175

Roell, T., Neuhäuser, R., Seifahrt, A., & Mugrauer, M. 2012, A&A, 542, A92

Rowe, J. F., Bryson, S. T., Marcy, G. W., et al. 2014, ApJ, 784, 45

Santerne, A., Hébrard, G., Deleuil, M., et al. 2014, A&A, 571, A37

Tokovinin, A. 2014, AJ, 147, 87

Veras, D., & Armitage, P. J. 2007, ApJ, 661, 1311

Vogt, S. S., Marcy, G. W., Butler, R. P., & Apps, K. 2000, ApJ, 536, 902

Vorobyov, E. I. 2013, A&A, 552, A129

Williams, J. G., & Faulkner, J. 1981, Icarus, 46, 390

Wisdom, J. 1980, AJ, 85, 1122

Zucker, S., Mazeh, T., Santos, N. C., Udry, S., & Mayor, M. 2004, A&A, 426, 695

Zucker, S., Naef, D., Latham, D. W., et al. 2002, ApJ, 568, 363